

# Remote Control of Reversible Localized Protein Adsorption in Microfluidic Devices

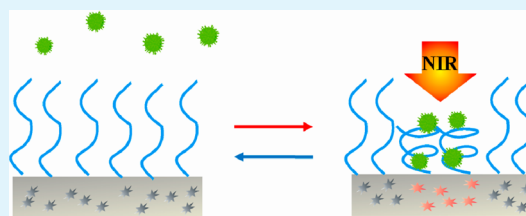
Nan Hao, Jin-Yi Li, Meng Xiong, Xing-Hua Xia, Jing-Juan Xu,\* and Hong-Yuan Chen\*

State Key Laboratory of Analytical Chemistry for Life Science, School of Chemistry and Chemical Engineering, Nanjing University, Nanjing 210093, China

## Supporting Information

**ABSTRACT:** We present a facilely prepared graphene oxide (GO)/poly(dimethylsiloxane) (PDMS) composite by dispersing nanosized GO in PDMS. On the basis of the combination of photothermal effects of GO and grafted thermoresponsive polymer, poly(*N*-isopropylacrylamide) (PNIPAAm), an optical-driving approach for remote control of localized wettability is realized. And this method has been successfully applied in the spatially controlled reversible protein adsorption in microfluidic devices.

**KEYWORDS:** protein adsorption, microfluidics, graphene, photothermal conversion, wettability



Microfluidics is a multidisciplinary platform and many interesting microfluidic devices have been designed over the years. Proper surface modification is vital to integrate multiple functions into one chip, especially in biology-related fields.<sup>1,2</sup> However, compared to the fast developing micro-fabrication techniques, the innovation in materials is limited. Various sophisticated 2D or 3D microstructure have been built, whereas the flexible control of localized surface property in the channel is still a hurdle. Lithographic process is a general approach to modify a microchannel with differentiation functionalized regions.<sup>3,4</sup> But lithography is expensive and cumbersome. Patterns based on lithography are predefined and irreversible, which is inconvenient to adjust during the experiment. As a result, facile prepared and simple operating methods for controlling the localized surface property of microchannels are of great significance.

Wettability (hydrophobic or hydrophilic) is an important property for solid surfaces both in fundamental research and industrial technologies,<sup>5,6</sup> such as self-cleaning surfaces, oil-water separation, microfluidic devices, liquid painting and bioadhesion, etc. Many materials possess switchable wettability. Environmental stimuli such as temperature, pH, light, ionic strength, and electric field would trigger the reversible wettability conversion by changing the surface structure or roughness at nanoscale.<sup>7–11</sup> PNIPAAm is a thermoresponsive polymer that has a low critical solution temperature (LCST) of 32 °C. It is hydrophobic above the LCST and hydrophilic below the LCST. As a representative of temperature-sensitive polymers, PNIPAAm has been widely applied in the reversible adsorption and release in microfluidic devices. Bunker's group utilized the excellently reversible wettability of PNIPAAm to adsorb and release proteins, such as human serum albumin (HSA), bovine serum albumin (BSA), cytochrome C, myoglobin, and hemoglobin.<sup>12</sup> In previous works, we built a replaceable enzymatic microreactor based on a smart 3D

macroporous PNIPAAm monolith fabricated by in situ spatially controlled photopatterning technology.<sup>13</sup> By utilizing synergistic effect of hydrophobic interactions and topographic interactions, Jiang's group have successfully constructed a unique thermoresponsive nanostructured surface to reversibly capture and release targeted cancer cells without damage.<sup>14</sup>

As a class of two-dimensional carbon nanomaterials, graphene and its derivative graphene oxide have attracted much attention in the past decade because of their unique physical and chemical properties.<sup>15–17</sup> Various promising applications in many areas have been reported including nanoelectronics, nanocomposite materials, energy research, catalysis, and biomedicine. Because of their ability to absorb light in the near-infrared (NIR) region (800–1300 nm), graphene can serve as optical heating elements and graphene-based hybrid materials have been intensively studied in cancer phototherapy in recent years.<sup>18–20</sup> Graphene possesses superior optical absorption and photothermal conversion, large surface area, maturity of mass production, and lower cost compared with other NIR photothermal agents, including gold nanomaterials and carbon nanotubes.

In this paper, we reported a facilely prepared graphene oxide/PDMS composite to realize optical heating and remote control of localized wettability. And this material was further applied in spatially controlled protein adsorption by laser activation in microchannels. Some efforts have been paid on optical heating composites.<sup>21–23</sup> Matteini's group exploited a method for dose- and spatial-controlled functional molecules release from photoactivated nanocomposite films to living cells and tissues.<sup>24</sup> But to our best knowledge, there are few reports on spatially controlled reversible adsorption driven by light in

Received: June 24, 2014

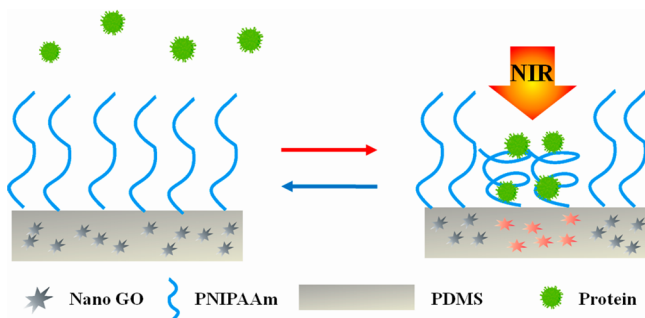
Accepted: July 28, 2014

Published: July 28, 2014

microfluidic devices. Compared to traditional Joule heating applied in microfluidics,<sup>25</sup> it is a noncontact approach and easy to use by avoiding the embedded and connection of electric circuits. Here we present a novel approach to achieve remote, spatially controlled protein adsorption.

First, we synthesized nanosized graphene oxide-poly(ethylene glycol) bis(amine) (NGO-PEG) and dispersed it in the PDMS prepolymer. The sizes of NGO-PEG sheets were lower than 50 nm according to atomic force microscopy (AFM) (see Figure S1 in the Supporting Information) and transmission electron microscope (TEM) (see Figure S2 in the Supporting Information) characterization, and the average thickness of NGO-PEG sheets were around 1 nm.<sup>26</sup> The detailed experimental process is provided in the Supporting Information. This mixture could be stored and used just like pristine PDMS prepolymer, which is easily cured in any shape or size with appropriate molds, avoiding the coating of additional heat layer.<sup>23,27</sup> From Figure S3 in the Supporting Information, we can see the D band (around 1300 cm<sup>-1</sup>) and G band (around 1600 cm<sup>-1</sup>) of graphene appeared among typical PDMS peaks. As shown in Scheme 1, the embedded NGO

**Scheme 1. Configuration Change of PNIPAAm on the Surface of GO/PDMS Composite with Exposure to a near Infrared (NIR) Laser, and the Following Protein Adsorption<sup>a</sup>**



<sup>a</sup>At room temperature (below 32°C), PNIPAAm presents a swollen hydrated state. When a laser beam illuminates this composite, embedded GO absorbs light energy and converts it to thermal energy to heat up the exposure region. After the temperature increases to LCST, H-bonding in the PNIPAAm breaks up and the hydrophobic interactions become predominant, which lead to a compact conformation with hydrophobic property and the reversible adsorption of proteins in the illuminated area.

functions as photothermal conversion materials due to its high light absorbing efficiency at the visible and near-infrared wavelengths. Switchable wettability is provided by PNIPAAm grafted via UV polymerization on the surface. At room temperature (below 32 °C), PNIPAAm presents a swollen hydrated state because of H-bonding formation between PNIPAAm chains and water molecules. When a laser beam illuminates this composite, embedded GO absorbs light energy and converts it to thermal energy to heat up the exposure region. After the temperature increases to LCST, H-bonding in the PNIPAAm breaks up and the hydrophobic interactions become predominant, which leads to a compact conformation with hydrophobic property. Then we got a small hydrophobic region among hydrophilic microchannels to adsorb hydrophobic molecules in water solution. NIR was chosen as the excitation laser because it is penetrating and harmless to

bioactive materials (excluding ultraviolet radiation), and will not cause possible photobleaching for common used fluorescence probe (exclude visible light).

We investigated the photothermal effect of GO/PDMS composite through experiments and simulations. Three samples with different GO concentrations of 0.25, 0.5, and 1 mg/g are shown in Figure 1a. The color changed from light brown to brown black. The transparency of these composites could be judged by the visibility of words under these samples. Transparency decreased clearly along with higher light absorbing efficiency. The first sample had a satisfying transparency, whereas words under the last sample are barely visible. We measured the temperature rise of exposure region on the GO/PDMS composite under a continuous laser illumination at 808 nm with a laser power density of 3.5 W/cm<sup>2</sup>. Blank PDMS is highly transparent and contributes little to the temperature increase after laser illumination.<sup>21</sup> As shown in Figure 1b, temperature variation is directly related with GO concentrations. For the sample of 1 mg/g, temperature at the illumination spot reaches around 60 °C from room temperature within 30 s. The temperature decreased to around 50 and 40 °C when GO concentration was reduced to 0.5 and 0.25 mg/g. To better understand the heat transfer process, we applied finite element numerical simulations in this system based on the heat transfer equation

$$\rho C_p \frac{\partial T}{\partial t} + \nabla(-k\nabla T) = Q$$

Where  $\rho$ ,  $C_p$ , and  $k$  are the density, heat capacity, and thermal conductivity of the material, respectively,  $T$  is the Kelvin temperature,  $t$  is time, and  $Q$  is the heat source power density. Detailed parameters are provided in the Supporting Information. Figure 1c shows simulation time–temperature curves. The time scale was extended to 500 s. Temperatures rise quickly in the beginning and then reach their maximum of 67, 83, and 104 °C, respectively, within minutes. It is noticeable that although the equilibrium temperatures differ a lot between three curves, they are all higher than LCST. As is well-known, the phase transition of PNIPAAm occurs in a narrow temperature range. Higher temperature contributes little to higher hydrophobicity. Because our intention is to implement remote control of localized wettability and spatial-controlled adsorption of hydrophobic materials, GO/PDMS composite of 0.25 mg/g performances well enough to realize this goal. The plateau of these curves indicates that heat generating from laser and heat transferring to surroundings reaches equilibrium. Heat transferring from illuminated region to surrounding areas is inevitable. It would decrease the temperature of exposure area. The warming of surroundings may also change the wettability of this area when temperature over LCST. This leads to the expansion of hydrophobic area and affects the precision spatial control. Surroundings included the external environment and the ambient composite. Figure 1d shows the temperature spatial distribution in an ideal open composite–water model after 5000 s of laser exposure to intuitively display this impact. Heat transfer in composite is limited because of the poor thermal conductivity of PDMS (0.15 W/(m K)) and good thermal conductivity of water (0.6 W/(m K)). More thermal energy is taken away by water, which leads to a restricted heating area. Compared to the composite–air system shown in Figure 1c, greater heat capacity and better thermal conductivity of water brings a lower equilibrium temperature (around 36 °C), which is in the range of physiological temperature. As

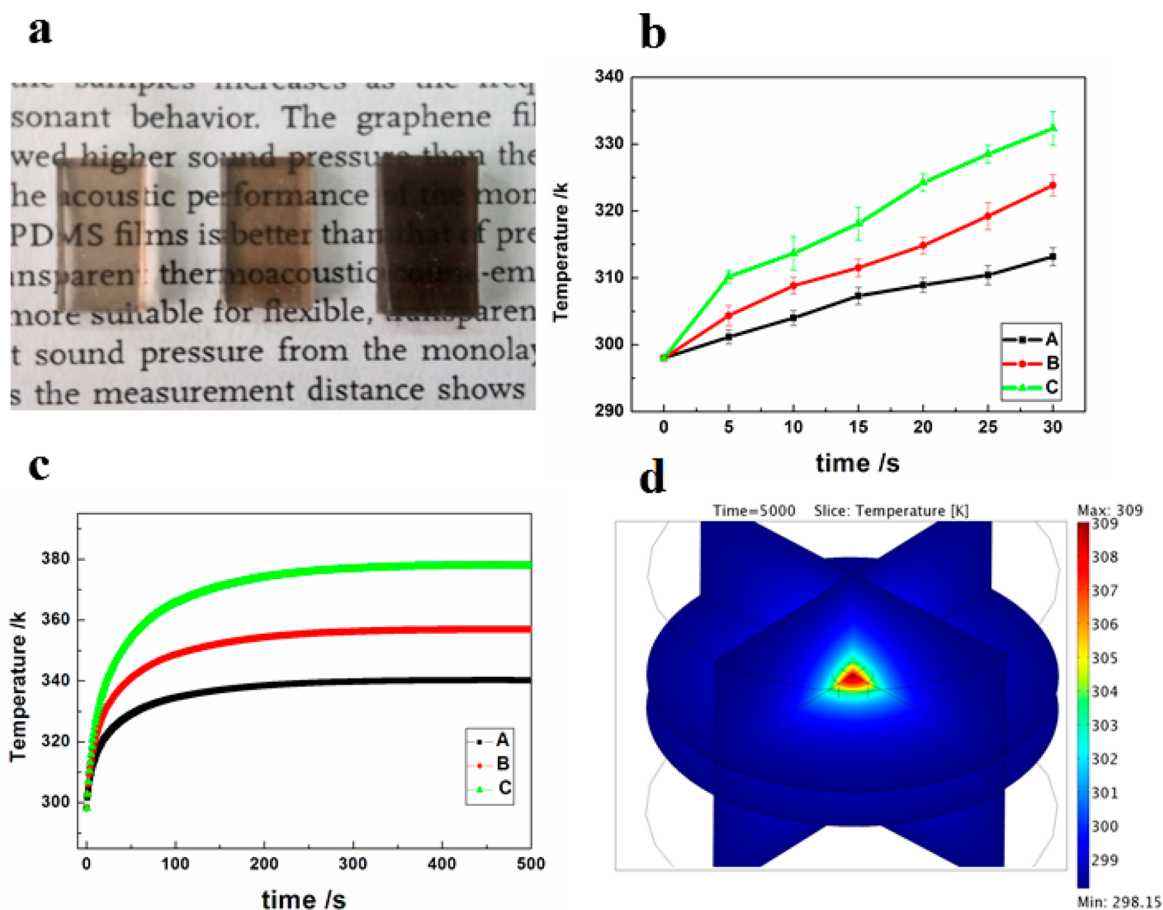


**Figure 1.** (a) Photograph of three GO/PDMS composites with different GO concentrations of 0.25, 0.5, and 1 mg/g. (b) Measured temperature–time curves of three samples: A (0.25 mg/g), B (0.5 mg/g), C (1 mg/g) exposure to NIR laser ( $3.5 \text{ W/cm}^2$ ). (c) Numerical simulations of the temperature–time curves. (d) Temperature spatial distribution in composite–water system.

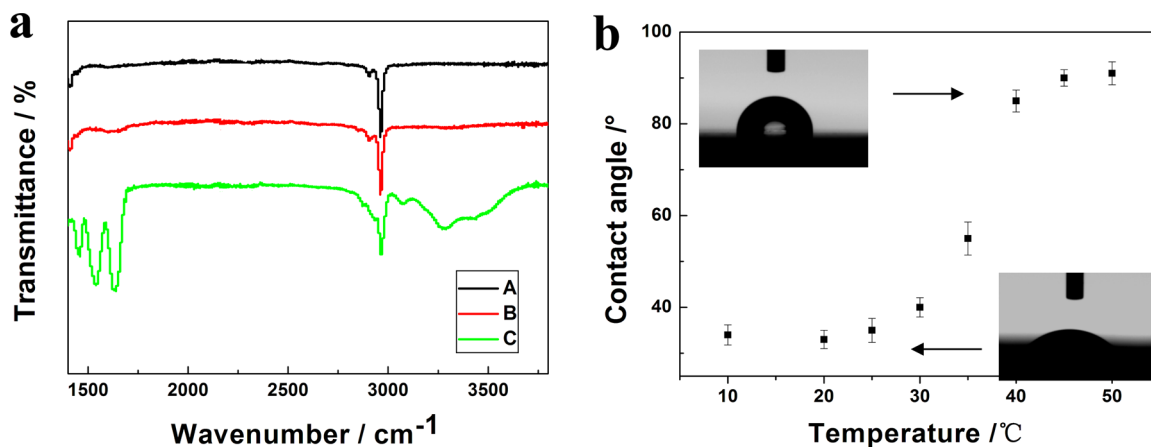


**Figure 2.** (a) ATR-FTIR spectra of the pristine (A) PDMS, (B) GO/PDMS composite, and (C) PNIPAAm grafted GO/PDMS. (b) Temperature dependence of water-contact angle for PNIPAAm-grafted GO/PDMS.

discussed above, this change has little effect on its hydrophobicity. On the other hand, lower temperature benefits the adsorption of bioactive molecules because of inhibiting the possible thermal denaturation of proteins or other biomolecules. In general, the temperature depended on the concentration of graphene oxide, the laser power, and the thermal exchange to environment. The final temperature could be regulated flexibly by adjusting these parameters. High concentration of graphene oxide is more favorable if trans-

parency is insignificant and great heat is needed. The possible following photothermal deoxygenation of graphene oxide in cured PDMS caused by laser illumination and high temperature would reduce transparency further.<sup>28</sup> For this experiment or other biology related applications, the temperature rised slightly from room temperature to  $37^\circ\text{C}$ . And the composite need to be transparent enough for on-chip optical analysis. So we chose the 0.25 mg/g sample to carry out the next step.

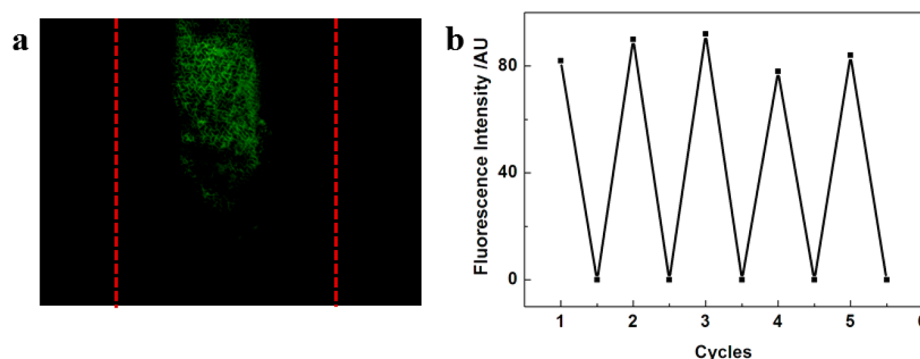


**Figure 3.** (a) Fluorescence image of the laser illuminated areas when irradiation time was 20 min. (b) Intensity analysis of cyclic adsorption and release experiments.

To graft PNIPAAm onto PDMS, we applied a well-studied UV-mediated polymerization procedure with benzophenone as initiator.<sup>29</sup> A gray film appeared on the surface after polymerization had been done. The thickness of polymers was around a few tens of nanometers, characterized by AFM (see Figure S4 in the Supporting Information). Pristine PDMS and GO/PDMS composite display nearly no difference in the Fourier-transform infrared absorption by attenuated total reflection spectra (ATR-FTIR) (Figure 2a). The grafted PNIPAAm film brings new strong absorbance peaks. The broad band at  $3300\text{ cm}^{-1}$  belonged to the N–H stretching vibrations for amide. The C=O stretching vibrations located at  $1630\text{ cm}^{-1}$ . The peak at  $\sim 1540\text{ cm}^{-1}$  can be assigned to N–H deforming vibration of the amide group.

PDMS is one of the most widely applied materials in microfluidic devices. It is stable, nontoxic and easy to process. But its highly hydrophobic surface is unfavorable. The grafting of PNIPAAm brings reversible wettability. The surface wettability is performed on a PNIPAAm-grafted PDMS using static water-contact angles measurements. As shown in Figure 2b, the surface exhibited a water-contact angle of about  $35^\circ$  when the temperature was below  $25^\circ\text{C}$ . When the temperature was above  $40^\circ\text{C}$ , the contact angle increased quickly to  $90^\circ$ , which indicated a thermally responsive switching between hydrophilicity and hydrophobicity. As Wu et al. has discussed, the transition time between extended state and collapse state of PNIPAAm is in the order of a few milliseconds.<sup>30</sup> So the wettability of the surface would change as soon as the temperature beyond LCST.

On the basis of the light controlled wettability of this GO/PDMS composite, we further tested its reversible protein adsorption/desorption in microfluidic system. Fluorescein isothiocyanate (FITC) labeled HSA was applied as a model. GO/PDMS composite had been incubated in chloroform overnight to remove residual curing agent and prepolymer inside the composite. The top layer of the microchip was made up of pristine PDMS while the bottom layer was GO/PDMS. They were bonding together after plasma treatment. And a wrinkled pattern was observed under microscope after the polymerization in the microchannel with a width of  $250\text{ }\mu\text{m}$  (see Figure S5 in the Supporting Information). Because the Si–H groups in the residual curing agent of pristine PDMS may deactivate photoinduced radical, PNIPAAm grafted on the bottom of the channel only. Fifty microliters of FITC-HSA ( $0.1\text{ mg/mL}$ ) was added in the inlet and the liquid flow was driven by gravity. We selected a random region in the channel and illuminated this area by laser for 20 min. Fluorescence image in

Figure 3a was captured after extra solution had been removed. The red lines represent the boundary of this channel. A fluorescent zone appeared while the rest was kept dark. This phenomenon demonstrates that the adsorption was directly correlated with laser illumination. As shown in Figure S6 in the Supporting Information, the disappearance of fluorescence indicated that the adsorbed protein could be released from the channel after flushed with cold water. The adsorption-release process occurred in a moderate condition and had no influences on the stability of proteins, PNIPAAm or GO/PDMS composite. The circular dichroism spectra of HSA after reversible adsorption and release and HSA with no treatment are shown in Figure S7 in the Supporting Information. Two negative bands at around 220 and 208 nm are respectively assigned to  $n-\pi^*$  transition and  $\pi-\pi^*$  transition of  $\alpha$ -helices. The fairly similar peak positions and intensities indicate the second structure of HAS is well-maintained. To investigate the reproducibility, we repeated the analysis for five cycles in the same microfluidic chip and the performance was stable (Figure 3b).

In conclusion, we have successfully prepared graphene oxide/PDMS composite to realize optical heating and control of localized wettability. Facilely prepared GO/PDMS composites possess the function of photothermal conversion while the advantages of pristine PDMS are well retained. The grafted PNIPAAm in situ brings thermoresponsive surface. This method could control the localized switch between hydrophobic and hydrophilic. Further, spatially controlled protein reversible adsorption in microchannels has been achieved successfully. The finely controlled wettability could be the basis of other modifications. It holds great potential in biomedicine and microfluidic areas, such as protein and cell pattern, bioadhesion, or biosensing.

## ■ ASSOCIATED CONTENT

### 📄 Supporting Information

Experimental details, including reagents and apparatus, synthesis of materials, simulation model, and additional characterization figures. This material is available free of charge via the Internet at <http://pubs.acs.org>.

## ■ AUTHOR INFORMATION

### Corresponding Authors

\*E-mail: [xujj@nju.edu.cn](mailto:xujj@nju.edu.cn). Tel/Fax: +86-25-83597294.

\*E-mail: [hychen@nju.edu.cn](mailto:hychen@nju.edu.cn). Tel/Fax: +86-25-8354862.

### Notes

The authors declare no competing financial interest.

## ■ ACKNOWLEDGMENTS

The authors are grateful for financial support from the 973 Program (Grants 2012CB933804) and the National Natural Science Foundation (Grants 21327902, 21135003, and 21121091) of China.

## ■ REFERENCES

- (1) Yoon, S.-H.; Chang, J.; Lin, L.; Mofrad, M. R. K. A Biological Breadboard Platform for Cell Adhesion and Detachment Studies. *Lab Chip* **2011**, *11*, 3555–3562.
- (2) Ronen, M.; Avrahami, D.; Gerber, D. A Sensitive Microfluidic Platform for a High Throughput DNA Methylation Assay. *Lab Chip* **2014**, *14*, 2354–2362.
- (3) Abate, A. R.; Krummel, A. T.; Lee, D.; Marquez, M.; Holtze, C.; Weitz, D. A. Photoreactive Coating for High-Contrast Spatial Patterning of Microfluidic Device Wettability. *Lab Chip* **2008**, *8*, 2157–2160.
- (4) Ghosh, A.; Ganguly, R.; Schutzius, T. M.; Megaridis, C. M. Wettability Patterning for High-Rate, Pumpless Fluid Transport on Open, Non-Planar Microfluidic Platforms. *Lab Chip* **2014**, *14*, 1538–1550.
- (5) Xin, B.; Hao, J. Reversibly Switchable Wettability. *Chem. Soc. Rev.* **2010**, *39*, 769–782.
- (6) Sun, A.; Lahann, J. Dynamically Switchable Biointerfaces. *Soft Matter* **2009**, *5*, 1555–1561.
- (7) Lim, H. S.; Kwak, D.; Lee, D. Y.; Lee, S. G.; Cho, K. Uv-Driven Reversible Switching of a Roselike Vanadium Oxide Film between Superhydrophobicity and Superhydrophilicity. *J. Am. Chem. Soc.* **2007**, *129*, 4128–4129.
- (8) Xu, L.; Chen, W.; Mulchandani, A.; Yan, Y. Reversible Conversion of Conducting Polymer Films from Superhydrophobic to Superhydrophilic. *Angew. Chem., Int. Ed.* **2005**, *44*, 6009–6012.
- (9) Wang, B.; Guo, Z. pH-Responsive Bidirectional Oil-Water Separation Material. *Chem. Commun.* **2013**, *49*, 9416–9418.
- (10) Casado-Montenegro, J.; Mas-Torrent, M.; Oton, F.; Crivillers, N.; Veciana, J.; Rovira, C. Electrochemical and Chemical Tuning of the Surface Wettability of Tetrathiafulvalene Self-Assembled Monolayers. *Chem. Commun.* **2013**, *49*, 8084–8086.
- (11) Wang, L.; Lin, Y.; Peng, B.; Su, Z. Tunable Wettability by Counterion Exchange at the Surface of Electrostatic Self-Assembled Multilayers. *Chem. Commun.* **2008**, 5972–5974.
- (12) Huber, D. L.; Manginell, R. P.; Samara, M. A.; Kim, B.-I.; Bunker, B. C. Programmed Adsorption and Release of Proteins in a Microfluidic Device. *Science* **2003**, *301*, 352–354.
- (13) Xiong, M.; Gu, B.; Zhang, J.-D.; Xu, J.-J.; Chen, H.-Y.; Zhong, H. Glucose Microfluidic Biosensors Based on Reversible Enzyme Immobilization on Photopatterned Stimuli-Responsive Polymer. *Biosens. Bioelectron.* **2013**, *50*, 229–234.
- (14) Liu, H.; Liu, X.; Meng, J.; Zhang, P.; Yang, G.; Su, B.; Sun, K.; Chen, L.; Han, D.; Wang, S.; Jiang, L. Hydrophobic Interaction-Mediated Capture and Release of Cancer Cells on Thermoresponsive Nanostructured Surfaces. *Adv. Mater.* **2013**, *25*, 922–927.
- (15) Huang, X.; Yin, Z.; Wu, S.; Qi, X.; He, Q.; Zhang, Q.; Yan, Q.; Boey, F.; Zhang, H. Graphene-Based Materials: Synthesis, Characterization, Properties, and Applications. *Small* **2011**, *7*, 1876–1902.
- (16) Liu, Y.; Dong, X.; Chen, P. Biological and Chemical Sensors Based on Graphene Materials. *Chem. Soc. Rev.* **2012**, *41*, 2283–2307.
- (17) Huang, X.; Qi, X.; Boey, F.; Zhang, H. Graphene-Based Composites. *Chem. Soc. Rev.* **2012**, *41*, 666–686.
- (18) Yang, K.; Feng, L.; Shi, X.; Liu, Z. Nano-Graphene in Biomedicine: Theranostic Applications. *Chem. Soc. Rev.* **2013**, *42*, 530–547.
- (19) Yang, K.; Zhang, S.; Zhang, G.; Sun, X.; Lee, S.-T.; Liu, Z. Graphene in Mice: Ultrahigh in Vivo Tumor Uptake and Efficient Photothermal Therapy. *Nano Lett.* **2010**, *10*, 3318–3323.
- (20) Li, M.; Yang, X.; Ren, J.; Qu, K.; Qu, X. Using Graphene Oxide High near-Infrared Absorbance for Photothermal Treatment of Alzheimer's Disease. *Adv. Mater.* **2012**, *24*, 1722–1728.
- (21) Fang, C.; Shao, L.; Zhao, Y.; Wang, J.; Wu, H. A Gold Nanocrystal/Poly(Dimethylsiloxane) Composite for Plasmonic Heating on Microfluidic Chips. *Adv. Mater.* **2012**, *24*, 94–98.
- (22) Geissler, M.; Voisin, B.; Clime, L.; Le Drogoff, B.; Veres, T. Thermo-Active Elastomer Composite for Optical Heating in Microfluidic Systems. *Small* **2013**, *9*, 654–659.
- (23) Jiang, L.; Erickson, D. Light-Governed Capillary Flow in Microfluidic Systems. *Small* **2013**, *9*, 107–114.
- (24) Matteini, P.; Tatini, F.; Luconi, L.; Ratto, F.; Rossi, F.; Giambastiani, G.; Pini, R. Photothermally Activated Hybrid Films for Quantitative Confined Release of Chemical Species. *Angew. Chem., Int. Ed.* **2013**, *52*, 5956–5960.
- (25) Fritzsche, F. S. O.; Rosenthal, K.; Kampert, A.; Howitz, S.; Dusny, C.; Blank, L. M.; Schmid, A. Picoliter Ndep Traps Enable Time-Resolved Contactless Single Bacterial Cell Analysis in Controlled Microenvironments. *Lab Chip* **2013**, *13*, 397–408.
- (26) Li, X.-L.; Shan, S.; Xiong, M.; Xia, X.-H.; Xu, J.-j.; Chen, H.-Y. On-Chip Selective Capture of Cancer Cells and Ultrasensitive Fluorescence Detection of Survivin Mrna in a Single Living Cell. *Lab Chip* **2013**, *13*, 3868–3875.
- (27) Cheng, X.; Yegan Erdem, E.; Takeuchi, S.; Fujita, H.; Ratner, B. D.; Bohringer, K. F. Infrared Light Induced Patterning of Proteins on Ppnipam Thermoresponsive Thin Films: A "Protein Laser Printer". *Lab Chip* **2010**, *10*, 1079–1085.
- (28) Abdelsayed, V.; Moussa, S.; Hassan, H. M.; Aluri, H. S.; Collinson, M. M.; El-Shall, M. S. Photothermal Deoxygenation of Graphite Oxide with Laser Excitation in Solution and Graphene-Aided Increase in Water Temperature. *J. Phys. Chem. Lett.* **2010**, *1*, 2804–2809.
- (29) Ma, D.; Chen, H.; Shi, D.; Li, Z.; Wang, J. Preparation and Characterization of Thermo-Responsive Pdms Surfaces Grafted with Poly(N-Isopropylacrylamide) by Benzophenone-Initiated Photopolymerization. *J. Colloid Interface Sci.* **2009**, *332*, 85–90.
- (30) Ye, X.; Lu, Y.; Shen, L.; Ding, Y.; Liu, S.; Zhang, G.; Wu, C. How Many Stages in the Coil-to-Globule Transition of Linear Homopolymer Chains in a Dilute Solution? *Macromolecules* **2007**, *40*, 4750–4752.